PHYSICAL REVIEW B **81**, 140402(R) (2010)

Coherent tunneling and giant tunneling magnetoresistance in $Co_2FeAl/MgO/CoFe$ magnetic tunneling junctions

Wenhong Wang,[1,2] Enke Liu,[2] Masaya Kodzuka,[1,3] Hiroaki Sukegawa,[1] Marec Wojcik,[4] Eva Jedryka,[4] G. H. Wu,[2] Koichiro Inomata,[1] Seiji Mitani,[1] and Kazuhiro Hono[1,3]

[1]*Magnetic Materials Center, National Institute for Materials Science (NIMS), 1-2-1 Sengen, Tsukuba 305-0047, Japan*

[2]*Beijing National Laboratory for Condensed Matter Physics, Institute of Physics, Chinese Academy of Sciences, Beijing 100080, People's Republic of China*

[3]*Graduate School of Pure and Applied Sciences, University of Tsukuba, Tsukuba 305-0047, Japan*

[4]*Institute of Physics, Polish Academy of Sciences, Al. Lotnikow 32/46, Warszawa 02-668, Poland*

(Received 8 January 2010; published 13 April 2010)

Spin-dependent coherent tunneling has been experimentally observed in high-quality sputtered-deposited $Co_2FeAl/MgO/CoFe$ epitaxial magnetic tunneling junctions (MTJs). Consequently, the microfabricated MTJs manifest a very large tunnel magnetoresistance (TMR) at room temperature and an unexpectedly TMR oscillation as a function of MgO barrier thickness. First-principles electronic band calculations confirm the pronounced coherent tunneling effect and are in good agreement with the experimental data. The present work demonstrates the importance of coherent tunneling for large TMR with Heusler alloys

DOI: 10.1103/PhysRevB.81.140402 PACS number(s): 75.70.Cn, 72.25.−b, 75.47.−m

Magnetic tunnel junctions (MTJs), which consist of two ferromagnetic electrodes separated by a thin tunneling barrier, are now considered as key components for next-generation spintronics devices because of their large tunneling magnetoresistance (TMR) effect.[1,2] Experimentally, progress toward devices with a large TMR ratio at room temperature (RT) has been motivated by using MgO tunneling barriers. Currently, there are two methods to achieve large TMR at RT. One is to use the half-metallicity of whole conduction electrons in half-metallic materials such as "selected" Heusler alloys (total band half-metallicity).[3–6] The other is to use the half-metallic Δ_1 band in certain metals (e.g., bcc Co and Fe) (Refs. 7 and 8) and alloys (e.g., CoFe and CoFeB) (Refs. 9 and 10) (specific band half-metallicity) due to coherent tunneling.[11,12] In earlier studies of TMR in MTJs consisting of Heusler alloy electrodes, main concern is to put on the former side.[13–21] Nevertheless, two contributions, i.e., their total band half-metallicity and coherent tunneling (specific band half-metallicity) were mixed in the obtained TMR. Therefore, a clear experimental observation of coherent tunneling in real Heusler-based MTJ devices is lacking. In this Rapid Communication, we report a giant TMR of 330–340 % at RT and its "remarkable" oscillation due to coherent tunneling in a disordered $B2$ Co_2FeAl Heusler alloy "without total band half-metallicity." This observation is further investigated and confirmed by first-principles electronic band calculations. Our work clearly indicates that besides bcc Co, Fe, and CoFe(B), Heusler alloys have promising potentials for giant TMR due to coherent tunneling as well as their tunable properties (such as magnetization and furthermore magnetic damping) based on a large variety constituent elements. In addition, Co_2FeAl has the lowest damping constant in Heusler alloys,[22] which is a substantial factor in spin dynamics such as spin injection magnetization switching with a low current. Our finding thus suggests that the Co_2FeAl-based MTJs may play a key role in future spintronics devices.

Thin films for spin-valve-type MTJs were prepared on Cr-buffered MgO(001) substrates using an ultrahigh vacuum magnetron sputtering system with the base pressure of below 8×10^{-8} Pa. The bottom Co_2FeAl (CFA) electrode was deposited at RT and subsequently annealed at 480 °C for 15 min in order to smooth its surface and to induce a perfectly flat bottom CFA/MgO interface. The structure of the annealed CFA layer has been found to be disordered $B2$ structure by using x-ray diffraction.[23] To further investigate the local environments around Co atoms, we have also measured ^{59}Co nuclear magnetic resonance (NMR). Figures 1(a) and 1(b) show ^{59}Co NMR spectra for CFA annealed at 480 °C after deposition on Cr- and MgO-buffered MgO(100) substrates and bulk CFA with $L2_1$ structure as a reference, respectively. The peak intensity around 193 MHz in the spectrum in Fig. 1(b) corresponds to the nearest-neighbor configuration of 4Fe+4Al around a Co atom in $L2_1$ structure. The satellite peaks with lower intensities suggest the existence of $B2$-type disordering, in which Fe and Al atoms swap.[24] The two spectra in Fig. 1(a) are quite different from the spectrum in Fig. 1(b) and show a perturbed $B2$ structure. The closer inspection of the spectra in Fig. 1(a) indicates that the structure corresponding to the CFA film grown on a Cr buffer is less resolved in high-frequency side than that of a film grown on an MgO-buffer layer, suggesting a less ordered $B2$ structure in the case of Cr buffer. The presence of a high number of resolved resonance lines in Fig. 1(a) suggests that in addition to the $B2$-type disorder some admixture of the $A2$-type disordering is also present in the CFA films. This may be attributed to the Co-rich composition of $Co_{52.8}Fe_{25.4}Al_{21.8}$ for the CFA film, which was found in the inductively coupled plasma analysis.

The MgO tunnel barrier was formed by rf sputtering directly from a sintered MgO target under an Ar pressure of 10 mTorr. As shown in Fig. 2(a), we designed a wedge-shaped MgO tunnel barrier layer with the MgO thickness (t_{MgO}) ranging from 1.0 to 2.5 nm on each 2×2 cm^2 substrate. The top CoFe electrode was then grown on the MgO tunnel barrier at RT, where CoFe means $Co_{75}Fe_{25}$ alloy. A 10-nm-thick

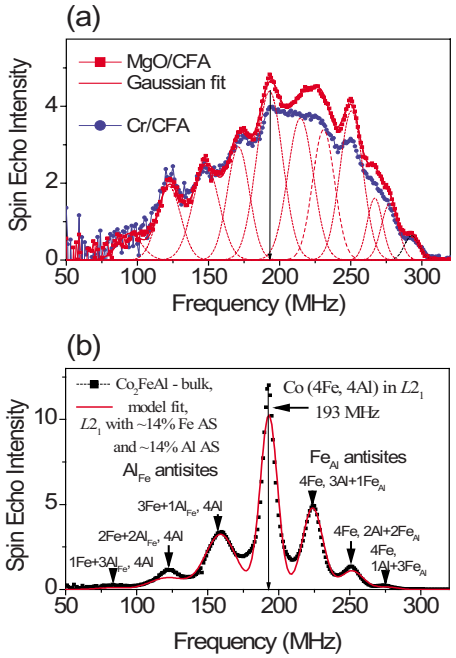

FIG. 1. (Color online) (a) ^{59}Co NMR spectra at 4.2 K for 30-nm-thick Co_2FeAl thin films *in situ* annealed at 480 °C after deposition on a Cr-buffered (blue) and MgO-buffered (red) MgO(100) substrates. The red solid line is Gaussian fit for each resonance peaks. (b) Spectrum for bulk Co_2FeAl with $L2_1$ structure. The peak intensity at 193 MHz corresponds to the nearest-neighbor atoms of 4Fe+4Al around a Co atom in $L2_1$ structure. The satellite structure extending symmetrically on both frequency sides of the main line reveals *B*2-type disordering, in which Al and Fe atoms are swapped.

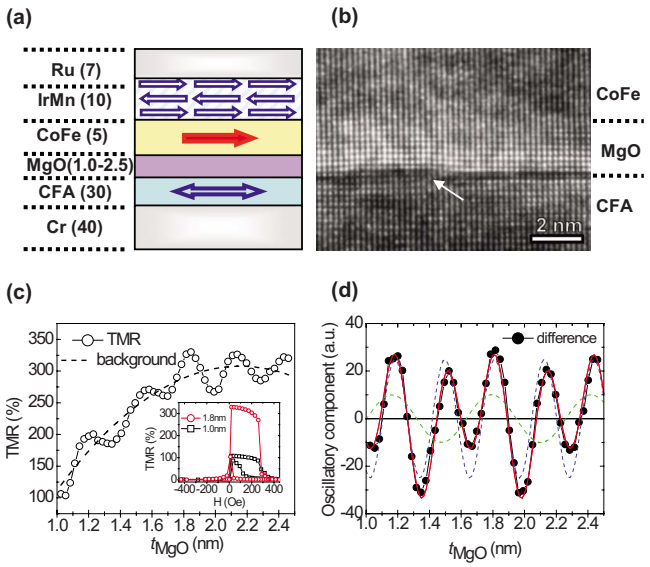

FIG. 2. (Color online) (a) Schematic of the magnetic tunnel junction structure. (b) High-resolution cross-section transmission electron microscopy images of an MTJ with t_{MgO}=2.0 nm. The vertical and horizontal directions, respectively, correspond to the MgO [001] and MgO [100] axis. The arrow in the micrograph shows the atomic step at the interface. (c) The MgO barrier thickness (t_{MgO}) dependence of TMR ratio at RT. Strong oscillation of TMR as a function of t_{MgO} is observed. Dashed green line represents background curve, which was fitted to quadratic function. (d) Oscillatory component of TMR, i.e., after subtracting the background as a function of t_{MgO}. The oscillatory component of TMR is fitted relatively well by superposing two cosine curves (solid red line) with different periods (λ): a short-period oscillation with λ =0.32 nm (dashed blue line) and a long-period oscillation with λ =0.63 nm (dashed green line).

IrMn antiferromagnetic layer was subsequently deposited on the top electrode in order to establish an exchange-bias field with the electrode. Lastly, the sample is capped with a 7-nm Ru layer. The structure of the fabricated MTJs was investigated by cross-sectional high-resolution transmission electron microscopy (HRTEM). A typical HRTEM image is shown in Fig. 2(b) for an MTJ structure with t_{MgO}=2.0 nm. This image clearly shows that all the layers from the CFA lower electrode to the CoFe upper electrode were grown epitaxially and were single crystalline. Although atomic steps can be seen at the lower interface, no appreciable lattice defects were observed inside the MgO barrier, which may be attributed to the small lattice misfit between CFA and MgO.[23] We should point out that the quality of the sputtered-MgO barrier is comparable with that of MgO barrier prepared by electron-beam method.[16,17,19]

Magnetotransport properties of the MTJ (junction area: 10×10 μm^2) have been measured by the standard dc four-probe method in a temperature range of 10–290 K, where a magnetic field was applied along CFA [110] (‖MgO[100]). Details of our microfabrication process and measurements are given in elsewhere.[23] In Fig. 2(c), we show the t_{MgO} dependence of observed TMR ratios. In this study, the TMR ratio is defined as $(R_{Ap}-R_P)/R_P$, where R_{Ap} and R_P are the tunnel resistance when the magnetizations of the two electrodes are aligned in antiparallel and parallel, respectively. The TMR of the MTJ is modest for thin MgO barrier but dramatically increases with increasing t_{MgO}. Notably, the highest TMR ratio of 330–340 % for CFA/MgO/CoFe MTJ is much higher than that of $Co_2FeAl_{0.5}Si_{0.5}$/MgO/CoFe MTJs (109% at RT) (Ref. 18) and Co_2MnSi/MgO/CoFe MTJs (217% at RT),[19] suggesting that the CFA electrode is more effective in enhancing the TMR effect.[25]

The most interesting result in Fig. 2(c) is that the TMR ratios of MTJ exhibit an unexpectedly oscillatory behavior as a function of t_{MgO}. The result is remarkable because such an oscillation of TMR is normally observed only in Fe/MgO/Fe MTJs prepared by molecular-beam epitaxy[7,26] while it is absent in sputter-deposited CoFe/MgO/CoFe (Ref. 9) and CoFeB/MgO/CoFeB (Ref. 10) MTJs. To get further insight into the physical origin of the result, as shown in Fig. 2(d), we replot the oscillatory component of TMR (i.e., after subtracting the background curve) as a function of t_{MgO}. We found that the oscillatory component of TMR is fitted relatively well by superposing two kinds of oscillations function (cosine curve) with different periods (λ): one of which is a short-period oscillation with λ=0.32 nm (dashed blue line) and the other one is a long-period oscillation with λ =0.63 nm (dashed green line). Moreover, the amplitude of the short-period is two times larger than that of the long-period one. It should be pointed out that the TMR oscillation observed in the Fe/MgO/Fe MTJ was also found to be a superposition of the short- (λ=0.32 nm) and long-period

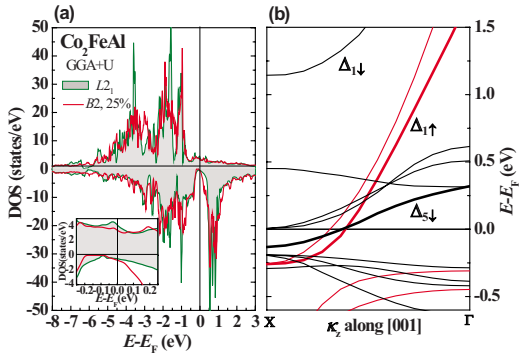

FIG. 3. (Color online) (a) Density of states of Co_2FeAl with the ordered $L2_1$ structure (green line) and with the disordered $B2$ structure (red line). Inset in (a) shows the magnification of DOS near the Fermi level (E_F). (b) Band dispersion of the disordered $B2$ Co_2FeAl along the [001] (Γ-X) direction. The red and black lines represent majority-spin and minority-spin bands, respectively. Overall three bands composed of two in the majority and one in the minority channel cross E_F. The thick red and thick black lines represent majority-spin Δ_1 and minority-spin Δ_5 bands, respectively.

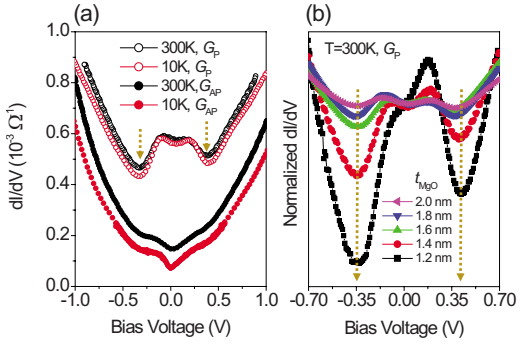

FIG. 4. (Color online) (a) Bias voltage dependence of differential conductance ($G=dI/dV$) spectra at 300 and 10 K for CFA/MgO/CoFe MTJ ($t_{MgO}=1.8$ nm). Here, the negative bias voltage corresponds to the tunneling of electrons from bottom CFA to top CoFe. P and AP stand for parallel and antiparallel alignment of the two electrodes. (b) t_{MgO} dependence of dI/dV spectra in the parallel alignment [$G_P(V)$] measured at 300 K. Each spectrum is normalized by the value at zero bias. The dark-yellow dotted arrows are guide to the eyes.

(λ=0.99 nm) oscillations. These results strongly indicate that the period of the oscillations is independent of electrodes and thus the origin of the oscillatory should only relate to the MgO tunnel barrier. Butler *et al.*[11] proposed a model of interference between tunneling states for the TMR oscillation in epitaxial Fe/MgO/Fe MTJs. An interference in the evanescent states at E_F in the MgO barrier between Δ_1 and Δ_5 states at $\boldsymbol{k}_\parallel=0$ can cause an oscillation of tunneling transmittance as a function of t_{MgO}, where $\boldsymbol{k}_\parallel=0$ is parallel components of the tunneling electrons wave vector. The tunneling transmittance for a given $\mathbf{k}_\parallel$ oscillates as a function of t_{MgO} with a period proportional to $1/(k_1\text{-}k_2)$, where k_1 and k_2 are real components of Δ_1 and Δ_5 states. Thus, we suggest that both the large TMR and its remarkable oscillation in CFA/MgO/CoFe MTJ may be originated from the coherent tunneling effect,[11,12] in which both the electrons' spins and their Bloch states symmetry are conserved. Nevertheless, there is much more to learn in order to fully understand the origin of TMR oscillation through further theoretical and experimental investigations.

To support the interpretation of our experimental results we have studied the band structure of disordered $B2$ CFA along the Γ-X ($\boldsymbol{k}_\parallel=0$) direction in the Brillouin zone. The calculations were performed using the pseudopotential method with plane-wave-basis set. The electronic exchange-correlation energy was treated under the local-density approximation for the experimental lattice constant of CFA, 0.572 nm. We used 120 κ points in the irreducible wedge of the Brillouin zone of the primitive cell and a plane-wave cut-off energy of 500 eV. These parameters ensure good convergences for total energy. Figure 3(a) shows the spin-resolved densities of states (DOS) of the ordered $L2_1$ (green line) and the disordered $B2$ (red line) CFA structure, respectively. In agreement with previous theoretical band predictions,[5,27] we found that: (i) there is no obvious peak in the majority-spin DOS at the Fermi level (E_F), both in the ordered $L2_1$ and the disordered $B2$ structure; (ii) compared to the ordered $L2_1$ system, a few additional states are found in the minority-spin DOS at E_F for the disordered $B2$ one [see inset of Fig. 3(a)]. This result has been explained by Galanakis[5] due to the strong hybridization between the Fe 3d and Co 3d, which will cause charge transfer from the Co minority-spin states to the Fe minority-spin states, and give rise to additional states at E_F and CFA loses half-metallicity. Moreover, within our calculation we found that the mixing of 25% Fe atom with Al atom (disordered $B2$) perturbs the symmetry of the Co and Fe sites creating new states at the conduction end of the band gap, which narrows the pseudogap considerably.

Figure 3(b) shows the band structure of the disordered $B2$ CFA along the Γ-X ($\boldsymbol{k}_\parallel=0$) direction. Overall three bands composed of two in the majority (solid lines) and one in the minority (dotted lines) channel cross E_F. From the symmetry analysis, surprisingly, we found that one of the majority-spin conduction bands (thick red line) has a Δ_1 (spd-like state) symmetry while the minority-spin conduction band (thick black line) has a Δ_5 (pd state) symmetry. Due to the symmetry compatibility with MgO band structure, the Δ_1 state has the smallest decay rate, followed by the Δ_5 state across the MgO barrier. One can therefore immediately confirm that the disordered $B2$ CFA along the [001] direction behaves as a half-metal in terms of the Δ_1 symmetry. Note that the band structure of CFA is quite similar to that of bcc Co,[28] but contrasts sharply with bcc Fe for which in addition to the Δ_1 band, there are other bands (Δ_2 and Δ_5) in the majority channel that cross E_F at $\boldsymbol{k}_\parallel=0$. This effect is, we speculate, the reason for the much larger TMR ratio for CFA/MgO/CoFe and Co/MgO/Co (Ref. 8) than Fe/MgO/Fe (Ref. 7) MTJs.

Figure 4(a) shows the bias voltage dependence of differential conductance ($G=dI/dV$) spectra of CFA/MgO/CoFe MTJs at 10 and 300 K. The small dip around zero bias observed in dI/dV spectrum for the antiparallel configuration [$G_{AP}(V)$] at 10 K is so-called "zero-bias anomaly" as usually observed in typical MTJs due to magnon excitations,[29] which disappears at 300 K. Slightly asymmetrical of dI/dV spectra

for the parallel configuration $[G_p(V)]$ with respect to the polarity of bias voltage was observed at both 10 and 300 K. The small asymmetrical feature probably reflects a slight different in the quality of the lower-CFA/MgO and the upper-MgO/CoFe interfaces in our MTJs as confirmed by HRTEM [see Fig. 2(b)]. It is interesting to note that, as marked by the arrows in Fig. 4(a), $G_p(V)$ spectra present a local minimum at about −0.35 and +0.38 eV for the negative and positive bias, respectively. This behavior is remarkable. To our best knowledge, such a conductance anomaly has not been observed in other Heusler-based MTJs. Here, we explain the local minimum by evoking the band dispersion of the disordered *B*2 CFA in the following way. As seen in Fig. 3(b), in fact the top of minority-spin Δ_5 band, which dominates the down spin conduction, lies at ~0.348 eV above E_F. When the energy of the conduction electrons arriving across the barrier overcomes the top of this Δ_5 band, the conduction channel associated with this state disappears. Therefore, the amplitude of the relative variation in $G_p(V)$ spectra from zero bias to the local minimum quantifies the contribution of the Δ_5 electrons in *P* channel conductivity. This interpretation remains in agreement with the results of Fig. 4(b) which show $G_p(V)$ spectra measured at 300 K for CFA/MgO/CoFe MTJs with various MgO barrier thicknesses. We clearly found the amplitude of the local minimum increases pronouncedly with decreasing the MgO barrier thickness (as indicated by dark-yellow dotted arrows). This important feature strongly indicates that the contribution of Δ_5 electrons to the tunneling becomes more significant in the thin MgO barrier thickness regime.

In conclusion, a new ferromagnetic electrode of the disordered *B*2 CFA Heusler alloy for pronounced coherent tunneling inducing giant TMR has been exploited. The micofabricated CFA/MgO/CoFe MTJ exhibits a very high TMR ratio of 330–340 % at RT and an unexpectedly TMR oscillation as a function of MgO barrier thickness. Additionally, a similar TMR oscillatory behavior was also observed in the CFA/MgO/CFA MTJs.[30] First-principles electronic band calculations confirm that the disordered *B*2 CFA along the [001] direction behaves as a half-metal in terms of the Δ_1 symmetry. The large TMR ratio together with the low damping constant of CFA suggests that this material may play a key role in future spintronics devices. Another important issue that we should point out is that the Heusler alloy of CFA we used includes considerable disorder, which strongly indicates that Heusler alloys have promising potentials for giant TMR due to coherent tunneling as well as their tunable magnetic properties (such as magnetization and furthermore magnetic damping) based on a large variety of constituent elements.

This work was partly supported by the NEDO, CREST, and JST-DFG. The work in Poland was partly supported by the Ministry of Sciences and Higher Education under Research Project No. 4531/B/T02/2010/38.

[1] J. S. Moodera, L. R. Kinder, T. M. Wong, and R. Meservey, Phys. Rev. Lett. **74**, 3273 (1995).
[2] T. Miyazaki and N. Tezuka, J. Magn. Magn. Mater. **139**, L231 (1995).
[3] R. A. de Groot, F. M. Mueller, P. G. van Engen, and K. H. J. Buschow, Phys. Rev. Lett. **50**, 2024 (1983).
[4] S. Ishida *et al.*, J. Phys. Soc. Jpn. **64**, 2152 (1995).
[5] I. Galanakis, P. H. Dederichs, and N. Papanikolaou, Phys. Rev. B **66**, 174429 (2002).
[6] S. Picozzi, A. Continenza, and A. J. Freeman, Phys. Rev. B **66**, 094421 (2002).
[7] S. Yuasa *et al.*, Nature Mater. **3**, 868 (2004).
[8] S. Yuasa *et al.*, Appl. Phys. Lett. **89**, 042505 (2006).
[9] S. S. P. Parkin *et al.*, Nature Mater. **3**, 862 (2004).
[10] D. Djayaprawira, Appl. Phys. Lett. **86**, 092502 (2005).
[11] W. H. Butler, X. G. Zhang, T. C. Schulthess, and J. M. MacLaren, Phys. Rev. B **63**, 054416 (2001).
[12] J. Mathon and A. Umerski, Phys. Rev. B **63**, 220403(R) (2001).
[13] K. Inomata *et al.*, Jpn. J. Appl. Phys. **42**, L419 (2003).
[14] Y. Sakuraba *et al.*, Appl. Phys. Lett. **88**, 192508 (2006).
[15] T. Ishikawa *et al.*, Appl. Phys. Lett. **89**, 192505 (2006).
[16] N. Tezuka *et al.*, Appl. Phys. Lett. **89**, 252508 (2006).
[17] T. Marukame *et al.*, Appl. Phys. Lett. **90**, 012508 (2007).
[18] W. H. Wang *et al.*, Appl. Phys. Lett. **92**, 221912 (2008).
[19] S. Tsunegi *et al.*, Appl. Phys. Lett. **93**, 112506 (2008).
[20] H. Sukegawa, W. Wang, R. Shan, T. Nakatani, K. Inomata, and K. Hono, Phys. Rev. B **79**, 184418 (2009).
[21] R. Shan, H. Sukegawa, W. H. Wang, M. Kodzuka, T. Furubayashi, T. Ohkubo, S. Mitani, K. Inomata, and K. Hono, Phys. Rev. Lett. **102**, 246601 (2009).
[22] S. Mizukami *et al.*, J. Appl. Phys. **105**, 07D306 (2009).
[23] W. H. Wang *et al.*, Appl. Phys. Lett. **95**, 182502 (2009).
[24] K. Inomata, M. Wojcik, E. Jedryka, N. Ikeda, and N. Tezuka, Phys. Rev. B **77**, 214425 (2008).
[25] We have measured the spin polarization (*P*) of the disordered *B*2 CFA film by point contact Andreev reflection method and found the value of $P=0.54$ at 4 K. According to Jullière's model, the TMR ratios for MTJs can be determined by the tunneling spin polarizations at E_F, P_1, and P_2 of the two electrodes, i.e., $\mathrm{TMR}=2P_1P_2/(1-P_1P_2)$. Within this model, the upper limit of the TMR values expected from MTJs using a CFA electrode will be 74%, if the other electrode is CoFe with $P=0.50$.
[26] R. Matsumoto *et al.*, Appl. Phys. Lett. **90**, 252506 (2007).
[27] Y. Miura, K. Nagao, and M. Shirai, Phys. Rev. B **69**, 144413 (2004).
[28] D. Bagayoko, A. Ziegler, and J. Callaway, Phys. Rev. B **27**, 7046 (1983).
[29] J. S. Moodera, J. Nowak, and R. J. M. van de Veerdonk, Phys. Rev. Lett. **80**, 2941 (1998).
[30] See supplementary material at http://link.aps.org/supplemental/10.1103/PhysRevB.81.140402 for a figure showing the oscillation of TMR in the CFA/MgO/CFA MTJs.